

Efficient NO Photodegradation of Hydrothermally Synthesized TiO₂ Nanotubes under Visible Light

Bui Dai Phat ¹, Tran Hong Huy ¹, Cao Minh Thi ², Pham Van Viet ¹

¹ University of Science, VNU-HCM

² Ho Chi Minh City University of Technology (HUTECH)

Abstract: In this study, TiO₂ nanotubes (TNTs) were synthesized via a hydrothermal process and characterized by high-resolution transmission electron microscopy (HR-TEM) images, selected area electron diffraction (SAED) pattern, and photoluminescence (PL) analysis. The NO removal photocatalytic activity of the hydrothermally synthesized TNTs was surveyed systematically. The hydrothermally synthesized TNTs have shown an efficient NO photodegradation which is approximately 4 times higher than that of P25 and an excellent photostability under visible light after 5 cycles. Furthermore, reactive radicals mainly involved in the photocatalytic reaction were identified by electron spin resonance (ESR) study, leading to a better understanding of the photocatalytic mechanism of the hydrothermally synthesized TNTs.

Keywords: TiO₂ nanotubes; NO removal; Photocatalysis; Trapping; ESR

1. Introduction

Nowadays, urban environments are facing serious problems concerning air pollution, mainly due to exhaust gases from traffic and burning fuels in industries, leading to a major environmental issue over the world. These negatively impacts on human health, animal life, plants and climate. There are two main air pollutant sources: natural sources, such as volcanic eruption, soil erosion, forest fires; and anthropogenic sources, in particular, emissions resulting from human actions^[1]. Therein, the latter is actually the most active cause of air quality degradation^[2]. Nitrogen(II) oxide and nitrogen(IV) oxide, both considered NO_x, are very harmful and poisonous gases emitted primarily from combustion^[3]. In addition, according to WHO's report, there are also natural environmental concerns in that air pollution also affects the survival and welfare of native flora and fauna. Furthermore, the built environment can be affected deleteriously through the effects of acid rain and fungal growth^[4]. Presently, the most common methods for the abatement of air pollutants are filtration and adsorption, such as electrostatic air purification, air filtration, and gas adsorption filtration^[5,6]. However, it may be noted that a potential shortcoming is that these methods involve physical removal and so require material replacement, cleaning, and disposal. In contrast, the potential to decompose pollutants can eliminate these additional requirements^[1]. Therefore, there is a critical need to develop an effective, safe, and inexpensive technique to decompose as wide a range of air pollutants as possible. Photocatalysis is one of the most promising methods owing to its potential value not only in addressing the worldwide energy shortage but also because of its eco-friendly merit and high efficiency for the remediation of NO_x at part-per-billion (ppb) levels^[3,7].

TNTs are well known as the perspective material for several applications such as photocatalysis, sensors, solar

Copyright © 2018 Bui Dai Phat *et al.*

doi: 10.18063/mrsr.v2i2.636

This is an open-access article distributed under the terms of the Creative Commons Attribution Unported License

(<http://creativecommons.org/licenses/by-nc/4.0/>), which permits unrestricted use, distribution, and reproduction in any medium, provided the original work is properly cited.

cells, etc^[8,9]. Therein, the role of TNTs as a photocatalyst for water treatment is detailly surveyed and full potential due to its long-term chemical and optical stability, strong oxidizing ability, nontoxicity, high electron mobility, and large bandgap^[8]. On the other side, very few reports have recently concerned about the photocatalytic activity of TNTs under visible light due to their wide bandgap. Therefore, there are many previous studies indicating the loading metal or doping non-metal elements onto or into TNTs for the reducing bandgap purpose of the composites^[10-13]. However, the synthesis of TNTs by a hydrothermal process has indicated that the structure of hydrothermally synthesized TNTs often exists many defects, such as oxygen vacancy (OV) defects, Ti³⁺ defects, etc^[14]. The presence of these defects helps to improve the photocatalytic activity of the hydrothermally synthesized TNTs through a formation new energy levels into the bandgap leading to extending photoresponse ranges which could be efficiently improved use this material in real application^[10]. Furthermore, previous studies were only focused on the dyes removal photocatalysis over the hydrothermally synthesized TNTs under UV light and almost NO photodegradation under visible light has not been investigated.

Based on above reasons, this work is conducted to study the NO photodegradation ability of the hydrothermally synthesized TNTs under visible light. This study also provides the knowledge into the NO photodegradation ability of the hydrothermally synthesized TNTs as verified reaction products, primary factors for enhancing photocatalytic activity had been studied and discussed with provided evidence.

2. Experimental

2.1 Chemicals and materials

Commercial TiO₂ powder (Merck, 99.99%), sodium hydroxide (NaOH, Merck, 99%), hydrochloric acid (HCl, China, ethanol (C₂H₆O), P25 (Merck, 99.99%), 5,5'-dimethyl-1-pyrroline-N-oxide (DMPO) (TCI Co.), and deionized (DI) water (Puris-Evo water system) were used without further treatment.

2.2 Preparation of TNTs

A preparation of the TNTs by a hydrothermal process was conducted according to the optimized parameters in our previous study^[15]. First, 1.7 g of commercial TiO₂ powder was dissolved in 157 mL of 10 M NaOH. The above mixture was transferred to a stainless autoclave and heated at 135 °C for 24 h. The resulting product was treated with HCl and washed with DI until pH 7 was reached. Then, the product was dried at 80 °C for 5 h.

2.3 Characterizations of TNTs

Morphology of the material was examined by HR-TEM images and SAED pattern was obtained by a Japan JEOL, JEM-2100F. PL measurement were carried out at room temperature using 325 nm as the excitation wavelength with a Horiba Jobin-Yvon Nanolog spectrophotometer equipped with a Xe lamp as the excitation source. ESR signals of reactive oxygen species (ROS) were detected on a Bruker EMX Plus X-Band spectrometer, which was generated in the photocatalytic process with radical spin-trapped reagent DMPO. The irradiation source was a high-pressure xenon short arc lamp (a Labguide® 150 W Mercury arc bulb lamp, $\lambda > 400$ nm). To reduce the experimental errors, the identical quartz capillary tube was used throughout the ESR measurement. Typical experimental conditions: temperature of 298 K, center field in 3483 G, sweep width with 200 G, frequency at 9.755 GHz, modulation amplitude at 1.00 G, and microwave power at 20 mW, the concentration of a sample at 400 ppm, 1000 ppm of DMPO.

2.4 Evaluation experiment of photocatalytic activity

2.4.1 Experimental system

The photocatalytic activity of as-prepared samples was evaluated by measuring the degradation ability of NO at ppb level in a continuous flow reactor at ambient temperature under visible light irradiation. The reaction chamber comprising a rectangular stainless- steel vessel (30 cm L × 15 cm W × 10 cm H) and covered with a quartz window. The visible light source was provided by a 300 W Xenon lamp (Perfect Light MICROSOLAR 300, Beijing, China) with a

UV cutoff filter ($\lambda > 420$ nm), which vertically passed through the quartz window. The measurement process was conducted as follows: First, the initial concentration of NO was obtained at 50 ppm from a compressed gas cylinder. Second, the concentration of NO was diluted to 450 ppb with an air stream supplied by a zero-air generator (Model 1001, Sabio Instruments LLC, Georgetown, TX, USA). The desired humidity level of the NO flow was kept at 70 % by passing the zero air streams through a humidification chamber. The gas streams were premixed completely by a gas blender, and the flow rate was controlled at 3 L.min⁻¹ by using a mass flow controller. In the photocatalysis process, after the catalyst achieved adsorption/desorption equilibrium, the Xenon lamp was switched on. Finally, the NO and NO₂ concentrations were continuously measured with a chemiluminescence NO_x analyzer (Model 42c, Thermo Environmental Instruments Inc., Franklin, MA, USA) during photocatalytic degradation at a sampling rate of 0.6 L.min⁻¹. The reaction between NO and air was negligible in the control experiment performed with or without light in the absence of the photocatalyst.

2.4.2 Photocatalytic activity test

For each photocatalytic activity experiment, one glass dish (d = 12 cm) containing the photocatalyst powder was placed at the center of the reactor. The photocatalysts were prepared by coating an aqueous suspension of the products onto a glass dish. The weight of the photocatalysts used for each experiment was maintained at 0.20 g. The dishes containing the photocatalyst were pretreated at 60 °C for several hours until the water in the suspension was completely removed. After that, the pretreated dishes were cooled to room temperature prior to the photocatalysis test. The removal efficiency of NO (η) and the yield of NO₂ (ψ) over different photocatalysts were calculated from Eqn. (1) and (2):

$$\eta (\%) = \frac{C_0 - C}{C_0} \times 100 \quad (1)$$

$$\psi (\%) = \frac{C_{NO_2}}{C_0 - C} \times 100 \quad (2)$$

where C is the NO concentration of the outlet at any one time, C₀ is the initial concentration of NO; and C_{NO₂} is the production of NO₂, ppbV.

The Langmuir-Hinshelwood (L-H) model has been used to determine the reaction rate constant for the photocatalytic reaction in both gas-phase and liquid-phase. To fit the experimental data, the adsorption can be reduced and the following linear form of Langmuir-Hinshelwood equation (Eqn. (3)) for the first-order reaction is used:

$$\ln \left(\frac{C}{C_0} \right) = -kt \quad (3)$$

where k is apparent reaction rate constant of ideal first order equation (min⁻¹) and t is photocatalytic reaction time (min).

3. Result and Discussion

3.1 TEM image analysis of hydrothermally synthesized TNTs

The morphology of the hydrothermally synthesized TNTs is tubular shapes with average length, outer diameter, and inner diameter of 263.47 nm, 9.59 nm, and 4.24 nm, respectively (**Figure 1(a)**). The distribution of the average length, outer diameter, and inner diameter of the hydrothermally synthesized TNTs was calculated by statistics of many TEM images at different magnifications (**Figure 1 (c)**). In addition, **Figure 1(b)** shows that the hydrothermally synthesized TNTs have the d-spacing of 0.35 nm and 0.23 nm, corresponding to the (101), and (200) lattice planes, respectively. SAED pattern of the hydrothermally synthesized TNTs is inserted in **Figure 1(a)** showed the presence of diffraction characteristics of (200) and (101) which is consistent with the HR-TEM result of the hydrothermally synthesized TNTs. These results demonstrated the formation of the TNTs synthesized by hydrothermal process.

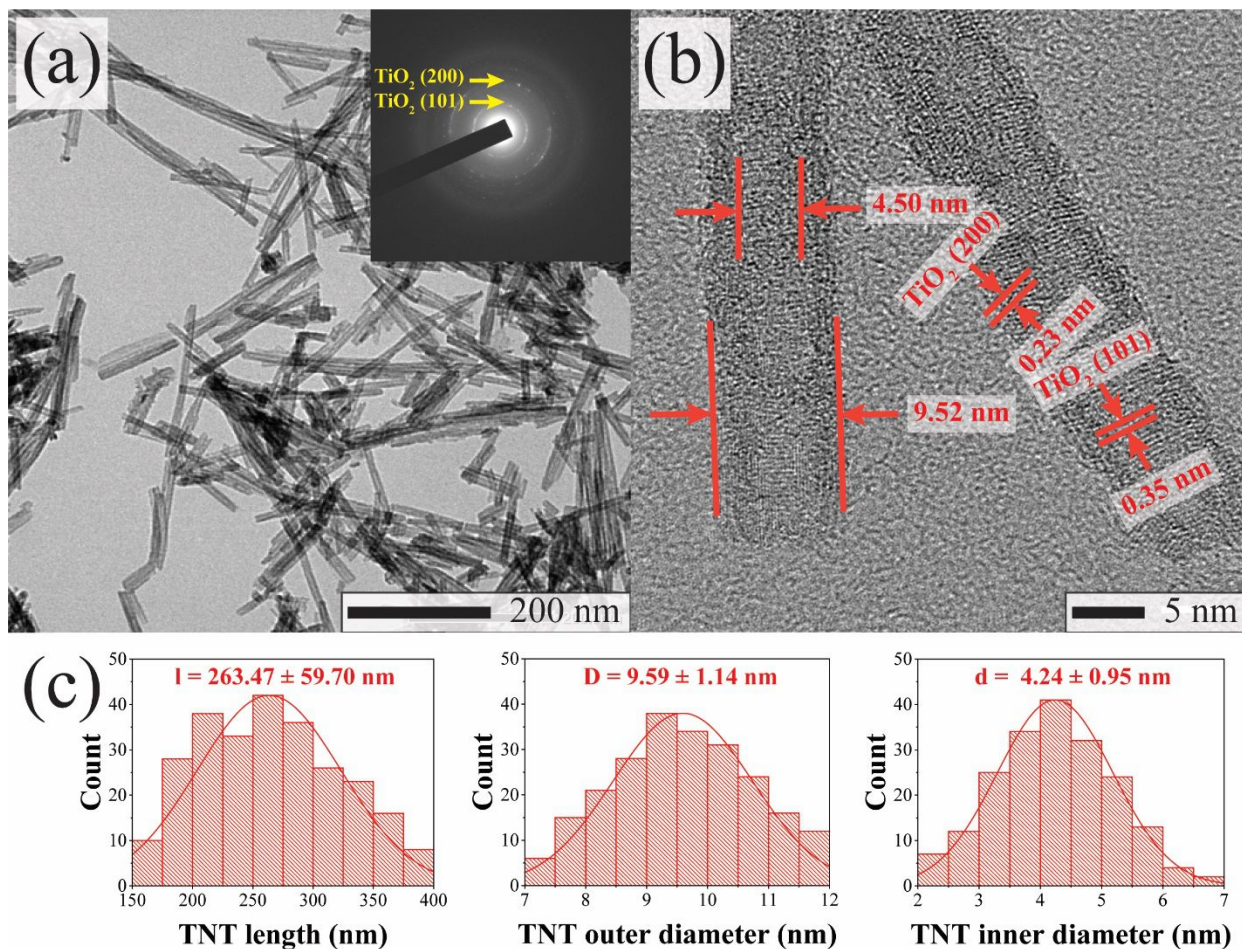


Figure 1; TEM images (a-b) with SAED pattern (inserted), and size distribution (c) of hydrothermally synthesized TNTs.

3.2 Photocatalytic activity of hydrothermally synthesized TNTs

The hydrothermally synthesized TNTs were surveyed for NO photodegradation under visible light irradiation and compared to that of P25 shown in **Figure 2**. Interestingly, the photocatalytic rate of the hydrothermally synthesized TNTs is superior compared to that of P25. This is shown by the photocatalytic rate for NO photodegradation of P25 in the first 5 min is low and remained constant for the rest of time. Meanwhile, in the case of the hydrothermally synthesized TNTs, the reactions showed no sign of leveling off during the entire of reaction time. To have an obviously quantitative comparison about the rate of NO photodegradation, L-H model was used to fit the experimental data (**Figure 2(b)**). The fitted results specify that the initial rate constant of the NO photodegradation over the hydrothermally synthesized TNTs were approximately 0.07 min^{-1} , 4 times higher than P25 (0.02 min^{-1}). Among these photocatalysts, the hydrothermally synthesized TNTs degraded 44.6 % NO under visible light in 30 min while P25 has an insignificant NO removal ability (11.6 %).

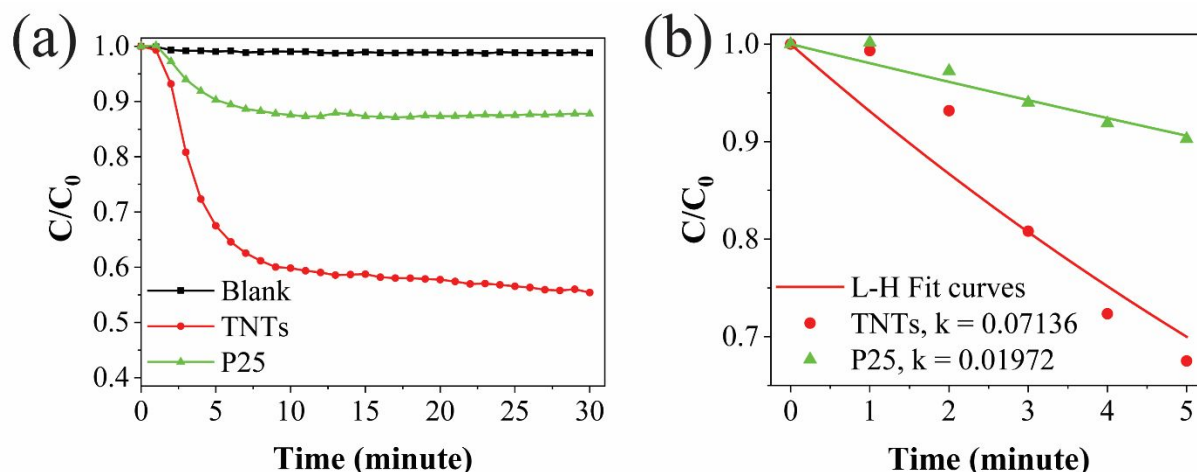


Figure 2; NO photodegradation activities of materials under visible light (a) and dependence of concentration versus irradiation time (b).

In order to determine the photostability of the hydrothermally synthesized TNTs, the recycle-ability of the hydrothermally synthesized TNTs was surveyed for the NO photodegradation in visible light for 5 cycles. **Figure 3(a)** shows that the NO photodegradation performance of the hydrothermally synthesized TNTs is highly stable. It shows the NO photodegradation efficiency of 44.6 %, 41.9 %, 36.3 %, 36.9 %, and 39.4 % corresponding to the first, second, third, fourth, and fifth cycle. This is concluded that the hydrothermally synthesized TNTs are stable in visible light.

In addition, to understand the primary factor of photocatalytic reaction, DMPO – ESR was measured and shown in **Figure 3 (b)**. The result indicated that superoxide anion radical is the key of the NO photodegradation with highly intensive peaks, which confirmed that electron was primarily involved in the photocatalytic reaction. Besides, the hydroxyl radical signal is not detected, revealing the hole is not the primary factor for the NO photodegradation.

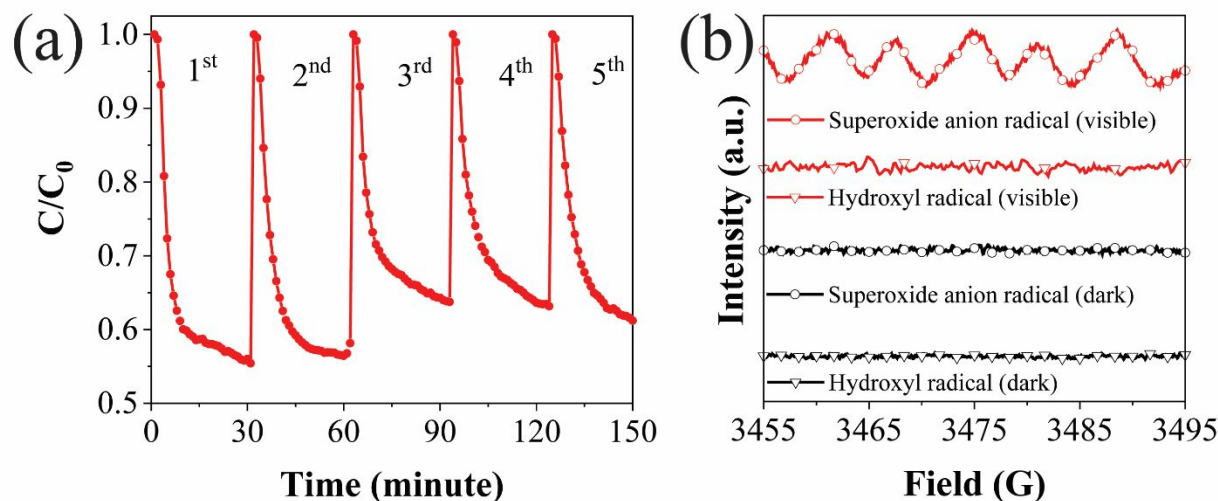


Figure 3; Photochemical stability (a) and DMPO-ESR spectra (b) of hydrothermally synthesized TNTs for DMPO- \bullet O₂⁻ and DMPO- \bullet OH.

3.3 NO photodegradation mechanism of hydrothermally synthesized TNTs

Figure 4 (a) shows PL spectrum of the hydrothermally synthesized TNTs with three emission peaks at 1.96 eV (632.5 nm), 2.36 eV (525.4 nm), and 2.83 eV (438.1 nm) corresponding to surface defects of Ti³⁺ or OVs, oxygen vacancies losing one electron (F⁺), and self-trapped excitons (STE) near the conduction band (CB) of TNTs, respectively^[10]. In addition, these defects can trap both electron and hole to significantly increase the carrier separation, resulting in a higher photocatalytic performance.

According to all the above information, the photocatalytic mechanism of the TNTs for the NO photodegradation can be described as following: the electron-hole pairs were generated when the TNT is irradiated by visible light (Eqn. (4)), then the photogenerated electrons favorably reduce O_2 to form O_2^- for the process of NO photodegradation (Eqn. (5-8)). Besides, the photogenerated holes partially oxidize H_2O to form $HO\bullet$ for NO removal (Eqn. (9-12) (**Figure 4** (b)))

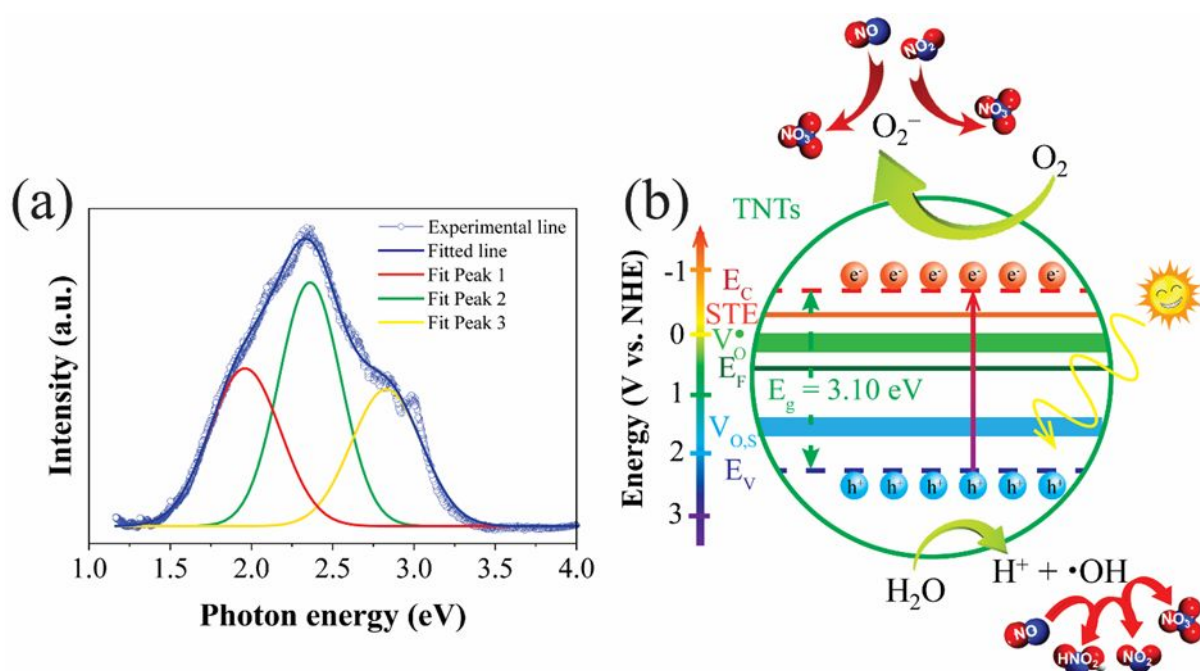


Figure 4; PL spectrum (a) and mechanism of NO photodegradation under visible light (b) of hydrothermally synthesized TNTs.

4. Conclusions

In summary, the NO photodegradation over the hydrothermally synthesized TNTs was systematically surveyed and exhibited that the NO photodegradation efficiency of the hydrothermally synthesized TNTs is more outstanding than that of P25. The generated electron plays a primary role for the NO photodegradation reaction of the hydrothermally synthesized TNTs under visible light. The superior performance promises a practical application ability of the hydrothermally synthesized TNTs for NO removal under the visible light as well as the platform for future studies in this field.

Acknowledgements:

This study was done with the support of The CM Thi Laboratory and The University of Science, Vietnam

References

1. Hangjuan Ren, Pramod Koshy, Wen-Fan Chen., *et al*, 2017, Photocatalytic materials and technologies for air purification. *J Hazard Mater*, 325, 340-366. DOI: 10.1016/j.jhazmat.2016.08.072.
2. Joana Ângelo, Luísa Andrade, Luís M.Madeira., *et al*, 2013, An overview of photocatalysis phenomena applied to NO_x abatement, *J Environ Manage*, 129, 522-39. DOI: 10.1016/j.jenvman.2013.08.006.
3. Janusz Lasek, Yi-Hui Yu, Jeffrey Wu, 2013, Removal of NO_x by photocatalytic processes, *J Photoch Photobio C*, 14, 29-52. DOI: 10.1016/j.jphotochemrev.2012.08.002.
4. WHO, 2010, WHO Guidelines for Indoor Air Quality: Selected Pollutants, in WHO Regional Office for Europe, Copenhagen.
5. Yiping Zhang, Jinhan Mo, Yuguo Li., *et al*, 2011, Can commonly-used fan-driven air cleaning technologies improve indoor air quality? A literature review. *Atmos Environ*, 45(26), 4329-4343. DOI: 10.1016/j.atmosenv.2011.05.041.
6. Bolashikov, Z.D. A.K. Melikov, 2009, Methods for air cleaning and protection of building occupants from airborne pathogens, *Build Environ*, 44(7), 1378-1385. DOI: 10.1016/j.buildenv.2008.09.001.
7. Danilo Spasiano, Raffaele Marotta, Sixto Malato., *et al*, 2015, Solar photocatalysis: Materials, reactors, some commercial, and pre-industrialized applications. A comprehensive approach, *Appl Catal B: Environ*, 170-171, 90-123. DOI: 10.1016/j.apcatb.2014.12.050.
8. Zhou, X., N. Liu, P. Schmuki, 2017, Photocatalysis with TiO₂ Nanotubes: “Colorful” Reactivity and Designing Site-Specific Photocatalytic Centers into TiO₂ Nanotubes, *ACS Catal*, 7(5), 3210-3235. DOI: 10.1021/acscatal.6b03709.
9. Manmadha Rao, Somnath Roy, 2014, Water assisted crystallization, gas sensing and photo-electrochemical properties of electrochemically synthesized TiO₂ nanotube arrays, *RSC Adv*, 4(90), 49108-49114. DOI: 10.1039/C4RA06842D.
10. Van Viet Pham, Hong Huy Tran, Xuan Sang Nguyen., *et al*, 2018, One-step hydrothermal synthesis and characterisation of SnO₂ nanoparticle-loaded TiO₂ nanotubes with high photocatalytic performance under sunlight, *J Mater Sci*, 53(5), 3364-3374. DOI: 10.1007/s10853-017-1762-6.
11. Van Viet Pham, Dai Phat Bui, Hong Huy Tran., *et al*, 2018, Photoreduction route for Cu₂O/TiO₂ nanotubes junction for enhanced photocatalytic activity, *RSC Adv*, 8(22), 12420-12427. DOI: 10.1039/C8RA01363B.
12. Van Viet Pham, Bach Thang Phan, Derrick Mott., *et al*, 2018, Silver nanoparticle loaded TiO₂ nanotubes with high photocatalytic and antibacterial activity synthesized by photoreduction method, *J Photoch Photobio A*, 352, 106-112. DOI: 10.1016/j.jphotochem.2017.10.051.
13. Van Viet Pham, Tan Sang Truong, Quoc Hien Nguyen., *et al*, 2018, Synthesis of a silver/TiO₂ nanotube nanocomposite by gamma irradiation for enhanced photocatalytic activity under sunlight, *Nucl Instrum Methods Phys Res B*, 429, 14-18. DOI: 10.1016/j.nimb.2018.05.023.
14. Liang-Bin Xiong, Jia-Lin Li, Bo Yang., *et al*, 2012, Ti³⁺ in the Surface of Titanium Dioxide: Generation, Properties and Photocatalytic Application, *J Nanomater*, 2012, 1-13. DOI: 10.1155/2012/831524.
15. Van Viet Pham, Bach Thang Phan, Van Hieu Le., *et al.*, 2015, The Effect of Acid Treatment and Reactive Temperature on the Formation of TiO₂ Nanotubes, *J Nanosci Nanotechnol*, 15(7), 5202-5206. DOI: 10.1166/jnn.2015.10025.